Talanta 105 (2013) 278–286

Contents lists available at SciVerse ScienceDirect

Talanta

journal homepage: www.elsevier.com/locate/talanta

Stump-like mathematical model and computer simulation on dynamic separation of capillary zone electrophoresis with different sample injections

Jie Zhang [1], Quan-Fei Huang [1], Jie Jin, Jiang Chang, Si Li, Liu-Yin Fan **, Cheng-Xi Cao *

Laboratory of Bioseparation and Analytical Biochemistry, State Key Laboratory of Microbial Metabolism, School of Life Science and Biotechnology, Shanghai Jiao Tong University, Shanghai 200240, China

ARTICLE INFO

Article history:
Received 21 June 2012
Received in revised form
22 September 2012
Accepted 5 October 2012
Available online 3 November 2012

Keywords:
Capillary zone electrophoresis
HVL model
Gaussian peak
Plateau peak
Simulation

ABSTRACT

In this paper, a novel mathematical model of stump-like peak was constructed for alternative computer simulation of capillary zone electrophoresis (CZE) by using Haarhoff–Van der Linde (HVL) function. Unlike a classical model of Gaussian peak, the developed model contains both Gaussian and plateau concentration distributions of analytes. Based on the model, the relevant computer software was developed and implemented in Borland Delphi 7 environment. The relevant results revealed that (i) the software could freely simulate the plateau and Gaussian distribution peaks; (ii) the simulator could simulate a dynamic process of CZE properly; and (iii) the program could display the final electropherogram of numerous analytes in CZE. We further conducted the relevant experiments and compared them with the simulations. The comparisons demonstrated the high agreement between the simulation results and the experiments as well as those cited from references. In addition, the software could calculate effective mobility, diffusion coefficient and concentration of analytes based on the physico-chemical parameters input by users. The developed model and software have evident significance for understanding of electrophoretic separation, conditional optimization and basic computation on physico-chemical parameters of analytes in CZE.

1. Introduction

Computer simulation is a powerful tool to display the vivid electrophoretic process and to economically provide the optimization on experimental conditions of electrophoretic separation [1]. Various mathematical models and their computer programs have been developed for simulations on isotachophoresis (ITP), isoelectric focusing (IEF), capillary zone electrophoresis (CZE) and online sample concentration in capillary electrophoresis (CE).

There have been numerous well-developed mathematical models and computer programs for ITP simulation so far. Beckers et al. in 1972 [2] advanced the simple model of ITP for computer simulation, with which up to eight metal ions can be visually and simultaneously separated in their given electrophoretic system. In 1984, Hirokawa [3] described a computer program for the simulation on ITP separation of fourteen lanthanoid metal ions using three electrolyte systems. Radi [4] in 1985 and Shimao [5,6] in 1986 advanced the numerical simulation for complex ITP systems (e.g., three systems and protein systems etc), revealing the behavior of ITP and counter ion components in the steady state of ITP. In 1992, Heinrich et al. [7] developed a versatile model and computer program for the rapid optimization of ITP (as well as CZE and continuous flow electrophoresis) conditions, such as buffer, ionic strength, temperature, Joule heat, activity coefficients and concentration, etc. Caslavska et al. [8] in 1993 performed a simple simulation of ITP evaluation using a commercial, inexpensive, computerized data acquisition system. In 1995, Schafer–Nielsen [9] advanced the time-based simulation of ITP with free definition on boundary conditions for handling n constituents with n pK-values and calculating constituent concentrations and derived parameters as a function of time. Schwer et al. [10] in 1993 described Simul 4 for the numerical simulation on ITP and Hruska et al. [11] further developed Simul 5 for the dynamic simulation of ITP on inspecting system peak, stacking analytes and optimizing separation conditions.

Almost at the same time, a series of IEF simulations have also been developed. In 1979, Murel et al. [12] developed a simple model and computer program for the illustration of pH gradient instability (e.g., drifting and plateau phenomena) in IEF run. During 1981–83, Bier et al. [1,13] advanced a steady state IEF model for the simulation on concentration profile, pH value, conductivity and potential gradient. They [14,15] in 1986 developed their software for the dynamics of IEF. In 2000, Mao et al. [16] developed a fine IEF program for the dynamics simulation with high resolution. With the assistance of the software, Mosher et al. [17] in 2002 restudied the post-separation stable phase in IEF and Thormann et al. [18,19]

* The first corresponding author: Prof. C.-X. Cao. Tel./fax: +86 21 3420 5820.
** The second corresponding author: Dr. L.-Y. Fan.
E-mail addresses: lyfan@sjtu.edu.cn (L.-Y. Fan), cxcao@sjtu.edu.cn (C.-X. Cao).
[1] The first two authors have equal contribution to the work.

0039-9140/$ - see front matter © 2012 Published by Elsevier B.V.
http://dx.doi.org/10.1016/j.talanta.2012.10.010

investigated the dynamics of protein during an IEF and pH gradient mobilization after steady-state IEF run. Shimao [20–22] also conducted the numerical simulation of protein separation in IEF, which was treated as zero velocity ITP. In 2009, Jin et al. [23,24] developed the mathematical model and software of moving reaction boundary (MRB), and further revealed the relation between IEF and MRB via the results of simulation and experiment.

Furthermore, various mathematical models and programs have been described for CZE simulation hitherto. In 1994–1999, Reijenga et al. [25] developed a computer program for the simulation on migration, dispersion of samples and the influence of different injection in CZE. Cifuentes and Poppe [26] in 1994 and Janine et al. [27] in 1999 performed the simulation of separation and mobility mapping of 58 peptides that varied in size from 2 to 39 amino acids and in charge from 0.65 to 7.82. Gas et al. [28] in 1995 simulated the peak dispersion, including wall absorption, and in 2002 they greatly developed the PeakMaster for the optimization of electrophoretic conditions (e.g., running buffer, pH value, concentration and electric field as well as effective length of capillary) in CZE [29]. Erny et al. [30] in 2001–2003 discussed how to use Haarhoff–Van der Linde (HVL) equation to simulate the peak in CZE. In 2008, Hsu and Hung [31] conducted the simulation of charged ion migration in CZE. Recently, Hruska et al. [32,33] extended the linearized model of electromigration by calculation of nonlinear dispersion and diffusion of zone and introduced a computer implementation of the mathematical model of CZE which can predict the shapes of the system peaks even for a complex injected sample profile, such as a rectangular plug.

Unlike the models of CZE mentioned above, this paper tried to propose a novel stump-like HVL mathematical model of electrophoresis which contains both Gaussian and plateau concentration distributions of analytes, to develop the relevant computer program for simulation on plateau peak and the dynamic separation process of CZE. At the same time, the relevant experiments were performed for the demonstrations on the validity of developed stump-like model and its relevant simulation results. The developed software supplies an alternative choice for computer simulation on CZE. Below are the developed HVL model, a versatile computer program, the dynamic simulation results and the relevant experimental demonstrations.

2. Theoretical

2.1. Mathematical model of peak

Fig. 1A shows an idealized Gaussian peak of analyte which can be quantitatively described by the HVL equation. Evidently, under the same conditions except sample injection, the model of Gaussian peak could not explain plateau peak in CZE which accompanied with long sample injection [24,33]. Fig. 1B reveals the modified HVL model, called as stump-like HVL model. As shown in Fig. 1, the Gaussian peak in Panel A is cleaved into two parts, viz., the left and right halves of a Gaussian peak. Then a rectangle peak is set between the left and right halves. As a result, a stump-like HVL model is created as shown in Panel B. The rectangle length is determined by sample injection time in CE. The whole stump-like HVL model symbolizes a plateau-like peak if an abundant sample injection is given. Obviously, the modified model turns into an idealized Gaussian peak when the injection time is short. Under the condition of Panel A, the original HVL equation is modified as [34]

$$f(t)=\frac{a_0}{a_2\sqrt{2\pi}}\exp\left[-\frac{1}{2}\left(\frac{t-a_1}{a_2}\right)^2\right] \tag{1}$$

where, a_0 is the area of peak ($a_0=\int_{-\infty}^{+\infty}f(t)dt$), a_1 is the center of peak ($a_1=\int_{-\infty}^{+\infty}t\times f(t)dt/a_0$), a_2 is the variance of peak ($a_2=\int_{-\infty}^{+\infty}\left(t-a_1\right)^2f(t)dt/a_0$), and t is a time variable and can be rewritten as a distance variable x via mathematical conversion.

Suppose cross-sectional area of capillary is S, the amount of analyte M in a simulation can be computed with

$$M=\int_{-\infty}^{+\infty}Sf(t)dt \tag{2}$$

Thus, a_0, a_1 and a_2 in Eq. (1) respectively become

$$a_0=\int_{-\infty}^{+\infty}f(t)dt=\frac{M}{S}=cL \tag{3}$$

$$a_1=\frac{L_{\text{eff}}}{E\left(\mu_{\text{eff}}+\mu_{eof}\right)} \tag{4}$$

$$a_2^2=2Dt \tag{5}$$

where, L is the total length of capillary, L_{eff} is the effective length of capillary, E is the electric field intensity, μ_{eff} is the effective mobility, μ_{eof} is the electro-osmotic flow (EOF) mobility, D is the diffusion constant, and c is the concentration of analyte.

If the simulation is to display dynamic separation process of analytes (see the bottom column in Fig. S1B), the variable is a displacement (x), rather than the time (t). If there is the condition of $x_{\text{center1}}<x_{\text{center}}<x_{\text{center2}}$, there appears a plateau peak. And the model of plateau peak ought to be described with

$$f(x)=\frac{\int_{-\infty}^{+\infty}f(x)dx}{a_2\sqrt{2\pi}}\exp\left(-\frac{(x-x_{\text{center1}})^2}{2{a_2}^2}\right) \tag{6}$$

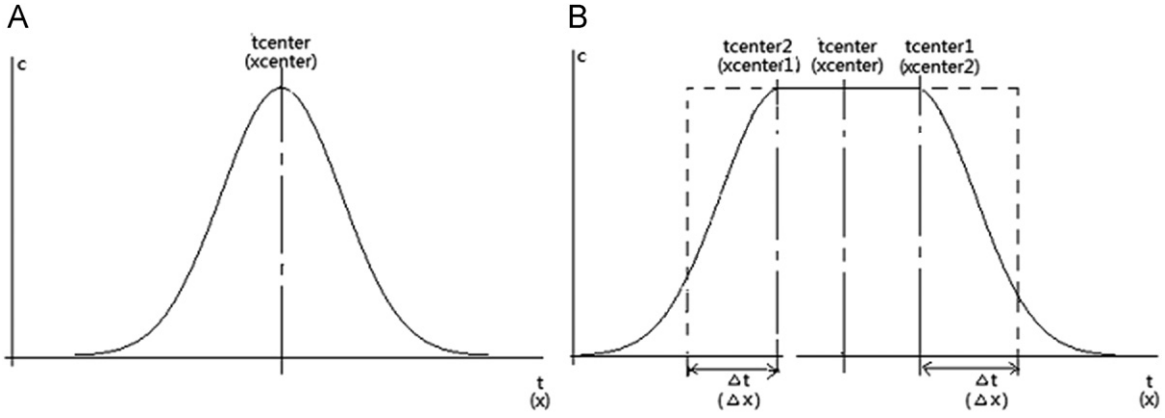

Fig. 1. Diagram of peak shape of Gaussian peak (A) and stump-like plateau peak (B). x-axis means running time (t) or distance from the inlet (x), y-axis means concentration of analytes.

$$\frac{2c\Delta x}{a_2\sqrt{2\pi}} = c \tag{7}$$

$$\Delta x = \frac{a_2\sqrt{2\pi}}{2} \tag{8}$$

$$x_{\text{center1}} = x_{\text{center}} - \left(\frac{L}{2} - \Delta x\right) \tag{9}$$

$$x_{\text{center2}} = x_{\text{center}} + \left(\frac{L}{2} - \Delta x\right) \tag{10}$$

If there is the condition of $x_{\text{center1}} = x_{\text{center}} = x_{\text{center2}}$, the center of peak becomes a point, and a Gaussian peak emerges. Evidently, the peak shape obeys Gaussian equation. The calculation of Gaussian peak is performed with the following equations:

$$f(x) = \frac{L \cdot c}{a_2\sqrt{2\pi}} \exp\left(-\frac{(x - x_{\text{center}})^2}{2a_2^2}\right) \tag{11}$$

$$x_{\text{center}} = E(u_{eff} + u_{\text{eof}})t \tag{12}$$

$$a_2 = \sqrt{2Dt} \tag{13}$$

Obviously, the simulation software not only simulates the dynamic process of analyte separation in CZE (see Eqs. (6)–(13) and the bottom column in Fig. S1B) but also simulates the electropherogram of analytes passing through detection window (see Eqs. (14)–(22) and the upper column in Fig. S1B). Hence, we use the time variable t to construct the mathematical model of peak shape. Note herein, t_{center}, t_{center1} and t_{center2} correspond with x_{center}, x_{center2} and x_{center1}, respectively. Variance a_2' caused by diffusion is the eigenvalues of peak, which has no relation with the plateau peak.

The value of t_{center} can be computed with

$$t_{center} = \frac{L_{eff}}{E(u_{eff} + u_{\text{eof}})} \tag{14}$$

$$a_2' = \frac{a_2}{E(u_{eff} + u_{eof})} \tag{15}$$

If there is the condition of $t_{\text{center2}} < t_{\text{center}} < t_{\text{center1}}$, there appears a plateau peak. And the model of plateau peak ought to be described with

$$f(t) = \frac{\int_{-\infty}^{+\infty} f(t)dx}{a_2'\sqrt{2\pi}} \exp\left(-\frac{(t - t_{center\ 1})^2}{2a_2'2}\right) \tag{16}$$

$$2c\Delta t = \int_{-\infty}^{+\infty} f(t)dx \tag{17}$$

$$\frac{2c\Delta t}{a_2'\sqrt{2\pi}} = c \tag{18}$$

$$\Delta t = \frac{a_2'\sqrt{2\pi}}{2} \tag{19}$$

$$t_{center\ 1} = t_{center} + \left(\frac{L}{2E(u_{\text{eff}} + u_{eof})} - \Delta t\right) \tag{20}$$

$$t_{center\ 2} = t_{center} - \left(\frac{L}{2E(u_{eff} + u_{eof})} - \Delta t\right) \tag{21}$$

When $t_{\text{center1}} = t_{\text{center}} = t_{\text{center2}}$, the peak shape obeys the Gaussian equation. The model of the Gaussian peak is described with Eqs. (17)–(21) and Eq. (22)

$$f(t) = \frac{Lc/E(u_{eff} + u_{eof})}{a_2'\sqrt{2\pi}} \exp\left(-\frac{(t - t_{center})^2}{2a_2'2}\right) \tag{22}$$

The model developed above, together with sample injection equation (Eq. (34)), is clearly different from the current mathematical modes of CZE, because it can freely simulate both a normal peak with Gaussian concentration distribution and a 'stump-like' peak with two halves of Gaussian and rectangle concentration distributions. In addition, the model can also freely imitate a transition state one between the two distributions under different sample injections (Sections 4.1 and 4.2). Hence, all of the simulations do not require the set of boundary conditions by a user, which is normally required in other softwares.

2.2. Calculation of pH value of background electrolyte (BGE)

The electro-neutrality equation of electrolytic solution is described as

$$f = \sum_{i=1}^{N} \sum_{z=n_i}^{p_i} zC_{i,z} + C_H - \frac{\kappa_w}{C_H} = 0 \tag{26}$$

where N is the number of solutes, z is the charge that ion carries, n_i is the lowest charge, p_i is the highest charge, C_H is the concentration of hydrogen ion, κ_w is the ion product constant of water, $C_{i,z}$ is the concentration of ion i that carries z electric charge. $C_{i,z}$ can be expressed using C_H

$$C_{i,z} = C_i \frac{1}{\sum_{z=n_i}^{p_i} Li,zC_{\text{H}}^z} L_{i,z}C_{\text{H}}^z \tag{27}$$

where C_i is the concentration of component i, $L_{i,z}$: is the parameter used to unify acid ionization and basic ionization. There was the following equation:

$$L_{i,z} = \begin{cases} \prod_{z=z}^{-1} K_{i,z'} & (z > 0) \\ \prod_{z'=1}^{z} \frac{1}{K_{i,z'}} & (z < 0) \\ 1 & (z = 0) \end{cases} \tag{28}$$

where, K is the dissociation constant of analytes, i means component i, z' means the valence state of the corresponding ion. There is no specific formula to solve Eq. (26), but Eq. (26) can be solved by the iterative method.

2.3. Calculation of system parameters

The ion concentration of each valence state is expressed as

$$C_{i,z} = C_i \frac{1}{\sum_{z=n_i}^{p_i} Li,zC_H^z} L_{i,z}C_H^z \tag{29}$$

The ionic strength (I) of BGE is computed with

$$I = \frac{1}{2}\left(\sum_{i=1}^{N} \sum_{z=n_i}^{p_i} C_{i,z}z^2 + C_{OH} + C_H\right) \tag{30}$$

The effective mobility of ion is computed with [35,36]

$$U_{N,\,eff} = \exp\left(-\eta\sqrt{zI}\right) \sum_{z=n_N}^{p_N} \text{sgn}(z)U_{N,z}\frac{C_{N,z}}{C_N} \quad \text{where } \eta = \begin{cases} 0.5 & |z| = 1 \\ 0.77 & |z| \geq 2 \end{cases} \tag{31}$$

where, sgn(z), which is a symbolic equation, symbols 1 when z is positive, and -1 when negative. And the conductivity can be

calculated with

$$\kappa = F\left(\sum_{i=1}^{N}\sum^{p_i}|z|U_{i,z}Ci,z + U_{OH}C_{OH} + U_H C_H\right) \quad (32)$$

The diffusivity coefficient is expressed as [16,17]

$$D_A = \frac{\mu_A kT}{z_A e} \quad (33)$$

where, k is the Boltzmann constant, T is the room temperature, viz. 298.15 K, e is the elementary charge, μ_A is the average effective mobility, and z_A is the average valence state.

2.4. Model of sample injection

Herein, the pressure sample injection induced by gravity is chosen for model of sample injection. The equation used for the sample injection is [37,38]

$$H = \frac{\Delta P r^2 t_{\text{inj}}}{32\eta L} \quad (34)$$

where, H is the length of sample injection, ΔP is the gravity-induced differential pressure between sample inlet and outlet of capillary, r is the inner diameter of capillary, t_{inj} is the injection time, η is the viscosity coefficient of buffer or sample (set at the viscosity of water).

3. Experimental

3.1. Reagents and Instruments

Monosodium phosphate (NaH_2PO_3, analytical grade reagent, AR), disodium hydrogen phosphate (Na_2HPO_3, AR), dimethyl sulfoxide (DMSO, AR), histidine (His, AR), hydrochloric acid (HCl, AR), and sodium hydroxide (NaOH, AR) were purchased from Shanghai Chemical Reagent Co. (Shanghai, China).

The experiments were performed with a capillary electrophoresis system (Beijing Cailu Scientific Instrument Factory, Beijing, China). The system consists of a power supply (up to 30 kV) with a current limit of 300 μA, an HW-2000 chromatography workstation (Qianpu Software Co. Ltd., Nanjing, China), and an UV–visible detector (190～740 nm, set at 248 nm). The temperature of system was controlled at 25 °C. A fused-silica capillary (purchased from the Factory of Yongnian Optical Fiber, Hebei, China) was used (total length 53 cm, 44 cm effective length, I.D. 75 μm). A 320 pH meter (Mettler-Toledo Instrument Ltd., Shanghai, China) was used to measure the pH value of buffers. A pure water system (SG Wasseraufbereitung and Regenerierstation, Fahrenberg, Barsübttel, Germany) was used to produce ultra-pure water with specific conductivity down to 0.055 μS cm^{-1}.

3.2. Solutions and samples

The BGE is phosphate buffer, which is prepared by 46.5 mM NaH_2PO_3 and 3.5 mM Na_2HP0_3. The sample is made up with 100 μM His and 0.01% DMSO: prepare 400 μM stock solution of His and 1% DMSO solution using ultra-pure water, and take 100 μL stock solution of His and 4 μL DMSO solution to be diluted by the phosphate buffer to 400 μL. DMSO is a neutral molecule with UV-absorbance, which can be used to indicate EOF in CE.

3.3. Procedure of CZE

A new capillary was rinsed with 1.0 M NaOH for 10 min, ultrapure water for 10 min, 1.0 M HCl for 10 min and running buffer for 20 min in order. The temperature in all runs was controlled at 25°C. The injection was done by gravity injection, and the pressure was 15 mbar. The injection times were 10 s, 20 s, 30 s, 40 s, 50 s and 60 s. After the sample injection, the CZE was conducted at 15 kV. The capillary was washed with the running buffer for 5 min between two adjacent runs.

In the computer simulation, 50 mM H_3PO_4 and 96.5 mM NaOH were inputted as BGE, which is actually equal to the experimental phosphate buffer; 2 mM His and DMSO were inputted as analyte and EOF marker, respectively. Capillary parameters of simulation were the same with the experimental conditions: 53 cm capillary length, 44 cm effective capillary length, 75 μm inner diameter of capillary and 15 kV Voltage. EOF mobility is 27×10^{-9} m^2 V^{-1} s^{-1}, which can be calculated from the retention time of DMSO in the CZE run mentioned above. The pH value of BGE measured by pH meter was pH 8.25, and the software's calculation gave a value of 8.33. 10 s, 20 s, 30 s, 40 s, 50 s and 60 s were respectively inputted as the injection time, 15 mbar inputted as the injection pressure.

4. Results and discussion

4.1. Simulation of 10 virtual compounds

To test the reliability of the software, 10 virtual compounds were picked up for demonstration of the developed software's validity, the parameters of which were only used for software demonstration, not necessarily corresponding with real compounds. The simulation results were shown in Fig. 2. Panels A and B show the simulating electropherograms with 1.0 mm and 3.0 mm sample injections. The comparative results between Panels A and B reveal that (i) when injection lengths are different while other conditions keep constant, the peak height will be adjusted in line with the sample injection lengths; (ii) Gaussian peaks exist in Panel A due to short sample injection, while plateau peaks are present in Panel B due to long injection; (iii) the height of Gaussian peak is generally less than the concentration of analyte in its original sample, while the height of plateau peak is equal to the original concentration; and (iv) when injection length increases, the separation efficiency is reduced. Similar conclusions can also be drawn from the simulating comparison between Panels C and D, except that both Gaussian and plateau peaks exist in Panel D. Through comparison of Panels A and C, one can observe that when effective capillary length increases, the peak width will increase due to long-term diffusion, which also causes several plateau peaks in Panel B to convert to Gaussian peaks in Panel D. These qualitative results mentioned above indicate the correct transformation from the mathematical model in Sections 2.1–2.4 to the computer program in Section 2.5.

The results of Fig. 2 manifest that the developed model and software can freely simulate both a normal peak with Gaussian concentration distribution under the condition of the short sample injection or low concentration and a 'stump-like' concentration distribution under the condition of long sample injection or high concentration. In addition, it is directly observed in Fig. 2D that the software can also freely mimic a series transition state peaks between the first and tenth peak under the different sample concentrations. The similar simulation will be also observed in Fig. 3 revealing the transient progress from a normal gaussian peak to a wide plateau peak under different sample injection conditions, and will be demonstrated by the experiments in Fig. 4.

4.2. DMSO and His peaks with different sample injections

Fig. 3 shows the simulation results of DMSO and His at 10 s, 20 s, 30 s, 40 s, 50 s, and 60 s sample injections, where the simulating conditions are the same with the experimental ones.

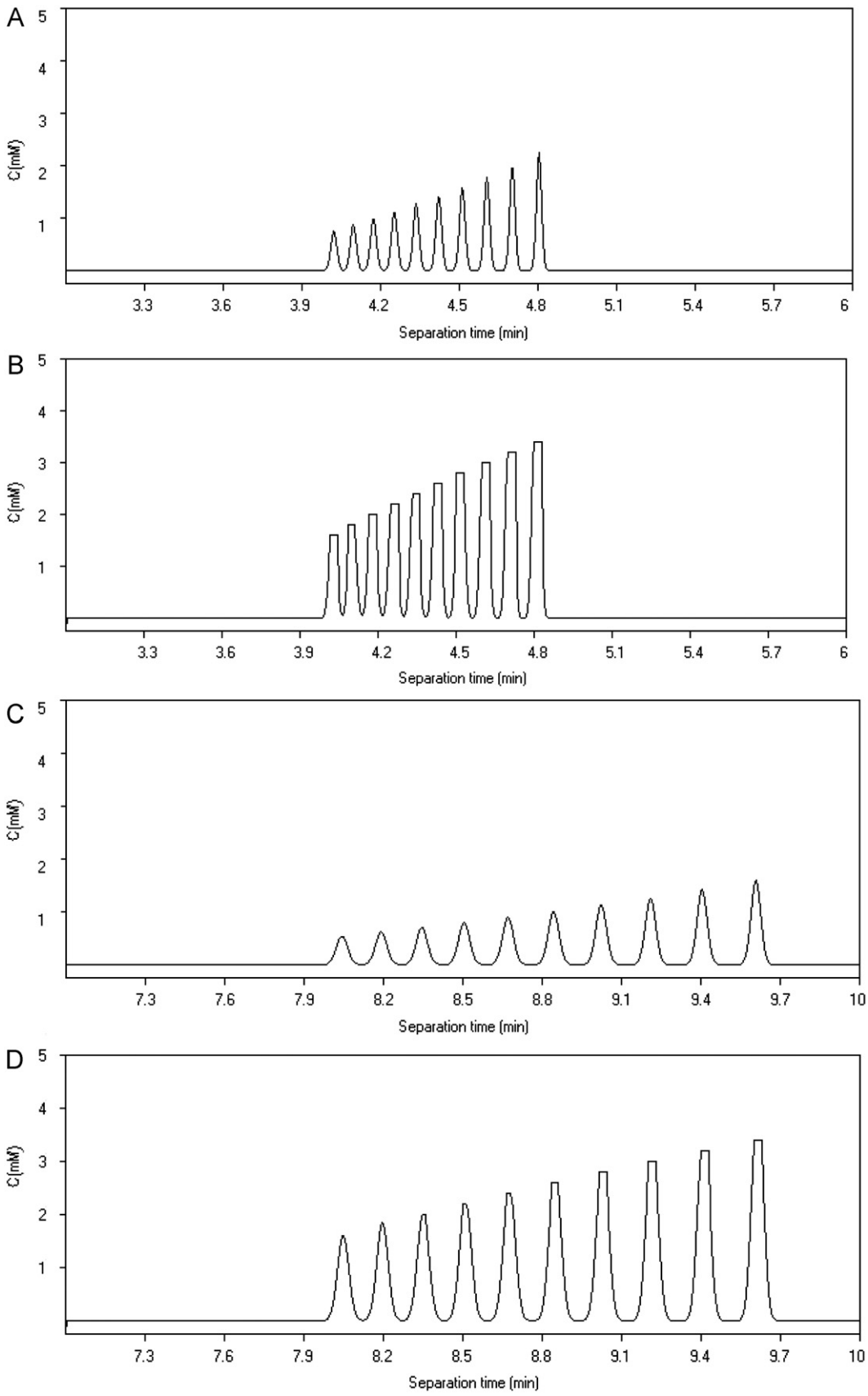

Fig. 2. Simulation electropherogram of 10 virtual analytes at 1.0 mm sample zone (A), 3.0 mm sample zone (B), 1.0 mm sample zone (C) and 3.0 mm sample zone (D). Simulation conditions: (i) BGE: virtual acid (c=20 mM, U(−1)=43 × 10^{-9} m^2 V^{-1} s^{-1}, $pK_a(-1)$ = 3.75) + virtual alkali (c=20 mM, U(+1) = 51 × 10^{-9} m^2 V^{-1} s^{-1}, $pK_a(+1)$ = 12); (ii) virtual analytes: their concentrations range from 1.6 mM to 3.5 mM with 0.2 mM interval, U(+1) range from 63 to 25 × 10^{-9} m^2 V^{-1} s^{-1} with 4 × 10^{-9} m^2 V^{-1} s^{-1} interval, $pK_a(+1)$=7; (iii) 20 kV; (iv) 20 × 10^{-9} m^2 V^{-1} s^{-1} EOF; (v) 45 cm total and 30 cm effective length capillary in Panel (A) and (B); (vi) 60 cm total and 45 cm effective length capillary in Panel (C) and (D).

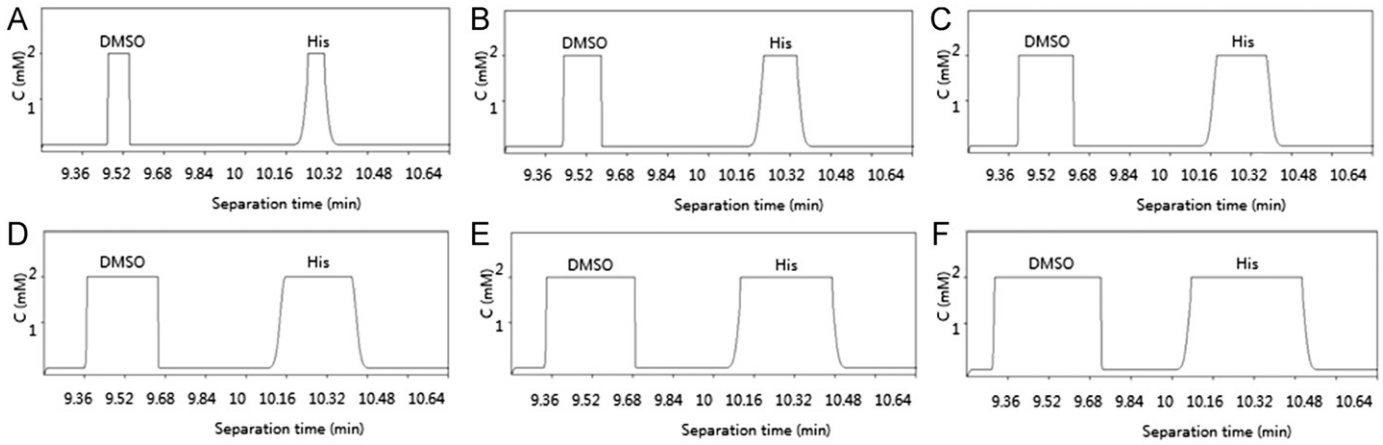

Fig. 3. Simulation electropherogram of DMSO and His with 10 s (A), 20 s (B), 30 s (C), 40 s (D), 50 s (E), and 60 s (F) sample injection. Simulation conditions: BGE: 50 mM H_3PO_4 and 96.5 mM NaOH, pH=8.33. Fifty three centimeter capillary length, 44 cm effective length, 15 kV driving voltage. EOF mobility: 27×10^{-9} m^2 V^{-1} s^{-1}.

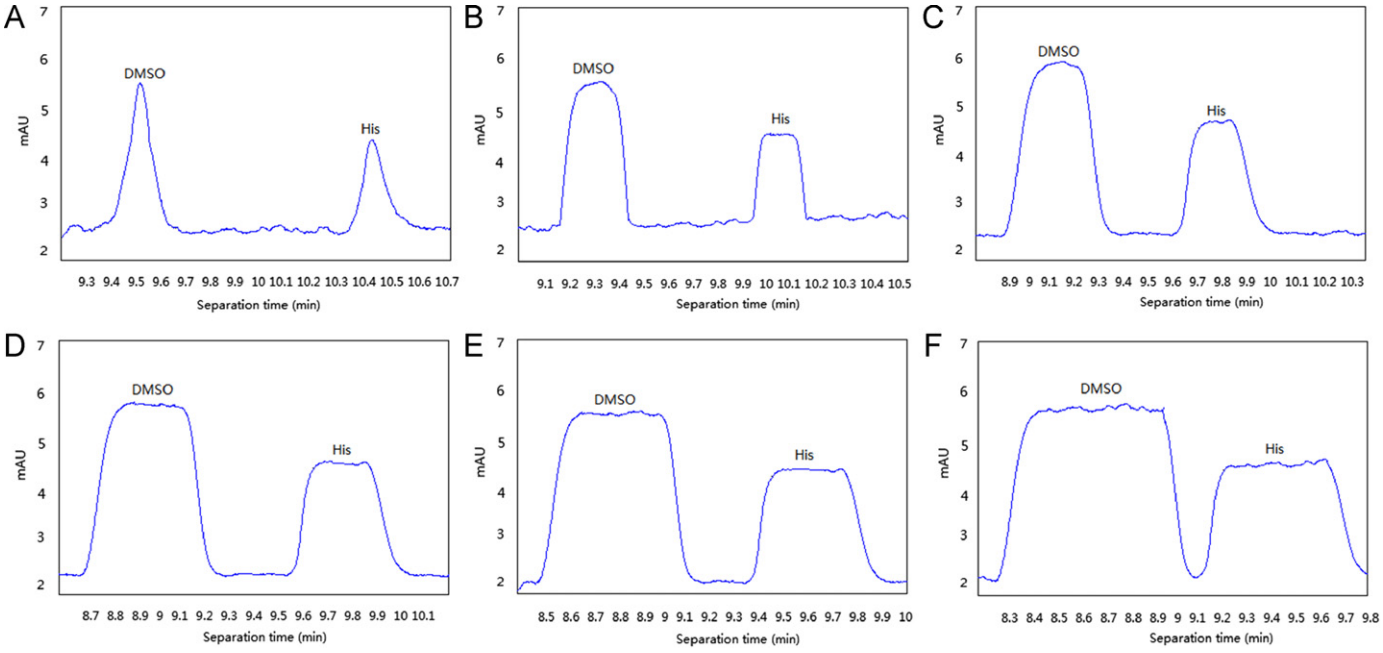

Fig. 4. Experimental electropherogram of DMSO and His with 10 s (A), 20 s (B), 30 s (C), 40 s (D), 50 s (E), and 60 s (F) sample injection. Experimental conditions: 50 mM pH 8.25 phosphate buffer used as the background buffer, 53 cm capillary length, 44 cm effective length, 15 kV driving voltage. Gravity injection at 15 mbar, 25 °C, 208 nm UV detection.

In Fig. 3 the plateau width of His increases gradually as injection time increases (Panel A–F). Fig. 4 shows the experimental electropherograms of DMSO and His in 50 mM pH 8.25 phosphate buffer under the conditions of 10 s, 20 s, 30 s, 40 s, 50 s, and 60 s sample injections. In Fig. 4A, the peak of His is a wide gaussian one, and from Fig. 4B to Fig. 4F the plateau width of His increases with prolonged injection time. The results of DMSO in Fig. 4 show similar altering tendency of these for His. In Table 1, the exact plateau widths in experimental and simulating electropherograms are given. There is an approximate linear relation between experimental plateau width and simulation plateau width (the linear equation is $y=0.5209x$, the corelation coefficient is $R^2=0.9921$). Evidently, the semi-quantitative comparisons between the simulations in Fig. 3 and the relevant experiments in Fig. 4 demonstrate the validity of developed stump-like mathematical model of CZE.

It is observed that the plateau widths in the simulation results of Fig. 3 are slightly higher than those in the experimental ones in Fig. 4 (Table 1). This may be induced by the following reasons.

Table 1
Comparisons of experimental and simulation results on the plateau width of His in Figs. 3,4.

	Injection time (s)					
	10 s	20 s	30 s	40 s	50 s	60 s
Zone width in Fig. 4 (s)	3.7	8.6	13.4	17.2	24.4	27.6
Zone width in Fig. 3 (s)	4.8	9.6	14.4	19.2	24.0	28.8

Firstly, the mathematical model of stump-like peak shape is simplified, and the viscosity of buffer, the temperature, the molecular size and the electromigration diffusion are not taken into the consideration of stump-like model. Secondly, the model of sample injection (Eq. (34)) can exactly describe the dynamic flow of mass solution in large tube, but may approximately predict the flow of micro-solution in capillary. Thirdly, there may be a deviation between the inner diameters of capillary used

in the experiments of Fig. 4 and the simulation of Fig. 3. Anyway, there is a high linear relation between the simulating and experimental results in Table 1, indicating the inner relationship between the simulations and experiments.

4.3. Simulations of 20 amino acids

Fig. 5 shows the comparison between the simulation electropherogram of 20 amino acids by the PeakMaster [28,29] and that via the developed stump-like software. The comparison reveals that there are no differences of peak sequences between the simulation results of the PeakMaster and stump-like software. It is further calculated that the electromigration time of 20 amino acids in the stump-like simulations is very close to that of the PeakMaster [28,29], the biggest variance between the two simulations is less than 10%. All of these results indicate a high agreement between the PeakMaster and stump-like simulations.

The simulations of 20 amino acids in Fig. 5 are further demonstrated by the relevant experiments by Komarova et al. [39]. In 2004, Komarova et al. [39] performed the separation of the underivatized amino acids in fodders and raw materials using CZE (Fig. R1). Evidently, the simulation results via both the stump-like and PeakMaster softwares are in general in agreement with the experimental results cited from Ref. [39] (Fig. R1). The experimental conditions of CZE [39] are the same as those of computer simulation in Fig. 5. Hence, one can quantitatively compare the electromigration times between the experiments [39] and the simulations in Fig. 5.

Table 2 displays the comparisons between the electromigration time of 20 amino acids in the experiments [39] and that achieved via the two software. From Table 2 it can be easily seen that peak sequences of experiments and computer simulation are nearly the same except the two amino acids of Pro and Tyr. Generally, if the electromigration time of analyte is relatively short, the deviation between experiments and simulation is rather small (except for Pro), and the relative deviation is less than 10%. As the electromigration time of analyte extends, the deviation also increases, and the relative deviation can be over 25% (such as Tyr, Glu and Asp). In the experimental results [39], the amino acid of Trp could not be detected. This may be caused by the amino acid in comigrating with other(s) (e.g., Val, or Gly, Leu and Ile).

The reason why there is over 25% deviation is still unclear completely. There may exist three reasons inducing the over 25% deviation. Firstly, there may be affinity interaction between the background buffer of borate (10 mM, pH 9.18) used in Ref. [39] and the amino acid (e.g., the hydroxyl group of Tyr), or charge interaction between the borate ion and amino group of amino acids (e.g., Pro, Glu and Asp). These interactions modified actual mobilities of amino acids (Pro, Tyr, Glu and Asp) which could be not considered in the developed software at present time. Consequently, the interaction resulted in the obvious deviation between the simulation and experiment. Secondly, the physical–chemical data of some amino acids used herein might be improperly measured in their references. As a result, there existed great deviation between the simulation and experiments of amino acids (Pro, Glu and Asp) [39]. It was further examined that the data of Pro, Tyr, Glu and Asp used herein were the same as those used in the PeakMaster [28,29]. Hence, there were high agreement between the simulative results of Tyr, Glu and Asp in Fig. 5A and those in Fig. 5B, but not the results of Tyr, Glu and Asp in Table 2 cited from Ref. [39]. In addition, the calculation of pH value in BGB (Section 2.2) is slightly different from others, especially the computation of ionic mobility with consideration on the influence of ionic strength (Eq. (31)) [35,36].

Fig. 6 gives a dynamic separation process of 20 amino acids in the capillary. As clearly shown in Fig. 6, the program can vividly simulate diffusion and distribution of these amino acids that are

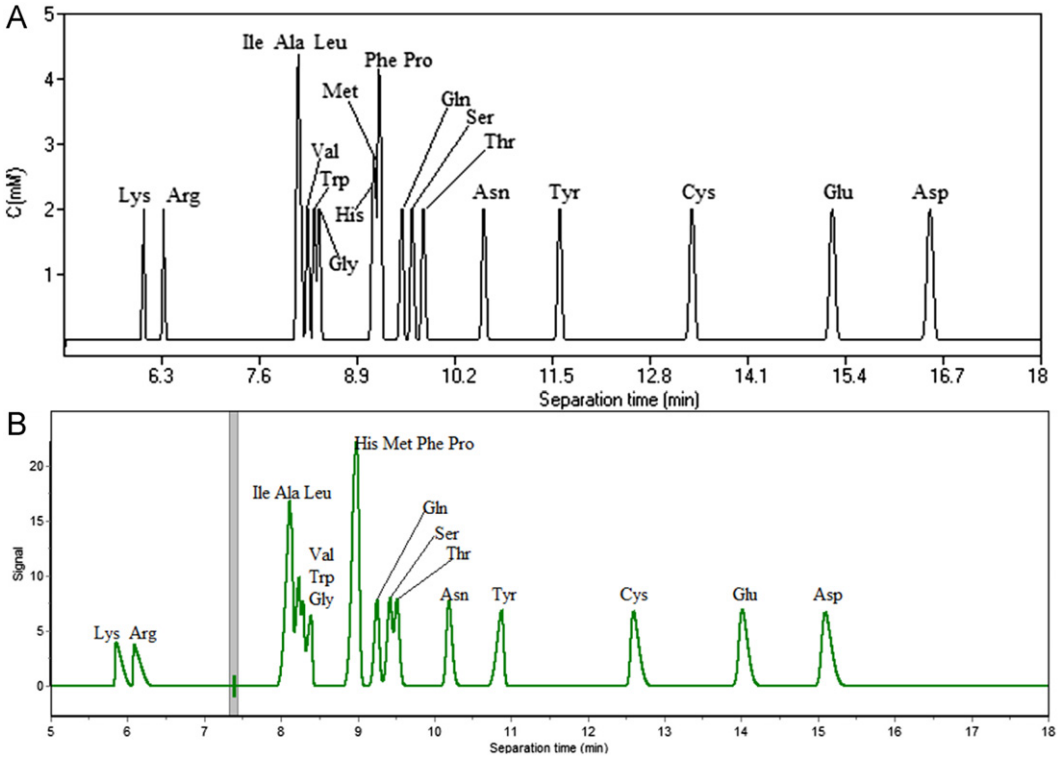

Fig. 5. Comparisons of simulation electropherogram between the developed software (A) and PeakMaster (B). Simulation conditions: BGE: 20 mM NaOH and 40 mM boric acid, 75 cm capillary length, 65 cm effective length, 20 kV driving voltage. EOF mobility: 55×10^{-9} m^2 V^{-1} s^{-1}, and sample injection length: 4 mm in Panel (A).

Table 2
Comparisons of experimental and simulation results on the electromigration time of 20 amino acids.

	Retention time (min)																		
	Lys	Arg	Pro	Ala	Val	Gly	Leu	Ile	Phe	His	Tyr	Met	Gln	Ser	Thr	Asn	Cys	Glu	Asp
Experiment[a]	6.1	6.2	7.5	7.7	7.8	7.9	7.9	7.9	8.4	8.4	8.5	8.6	8.7	8.8	9.1	9.6	11.5	12.6	13.3
PeakMaster[b]	5.9	6.1	9.0	8.1	8.2	8.4	8.1	8.1	9.0	9.0	10.9	9.0	9.3	9.4	9.5	10.2	12.6	14.0	15.1
Relative deviation[c]	3.3%	1.6%	20.0%	5.2%	5.1%	6.3%	2.5%	2.5%	7.1%	7.1%	28.2%	4.6%	6.9%	6.8%	4.4%	6.2%	9.6%	11.1%	13.5%
Stump-like[d]	6.0	6.3	9.2	8.1	8.2	8.4	8.1	8.1	9.2	9.1	11.6	9.1	9.5	9.6	9.8	10.6	13.3	15.2	16.5
Relative deviation[e]	1.6%	1.6%	22.7%	5.2%	5.1%	6.3%	2.5%	2.5%	9.5%	8.3%	36.5%	5.8%	9.2%	9.1%	7.7%	10.4%	15.6%	20.6%	24.1%

[a] The experimental time of electromigration of amino acids were cited from [39].
[b] The electromigration time of 20 amino acids were simulated by PeakMaster [29].
[c] The relative deviation between the experiments and the PeakMaster simulation is calculated with: $|t_{Exp}-t_{Peak\ Master}|/t_{Exp}$.
[d] The electromigration time of 20 amino acids were simulated by the developed software.
[e] The relative deviation between the experiments and the stump-like simulation is computed with: $|t_{Exp}-t_{Sandwich\text{-}like}|/t_{Exp}$.

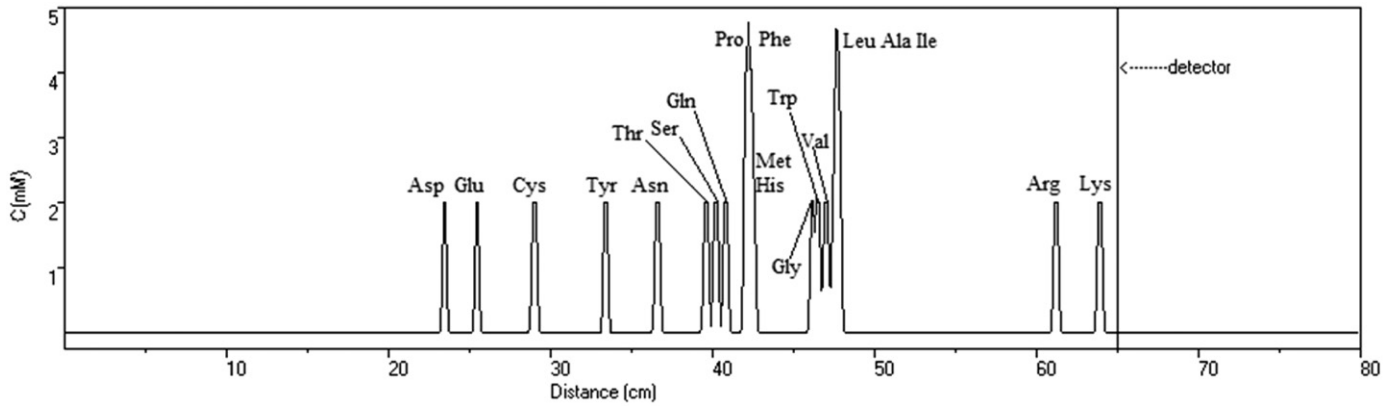

Fig. 6. Simulation electropherogram of dynamic separation process of 20 amino acids via the sandwich- like simulator. The simulation conditions are the same as those in Fig. 5A.

migrating through the capillary. From this electropherogram, it can be observed that no amino acid has reached the detector, but most of these amino acids have been separated.

5. Conclusions

From the simulation and experimental results, one can at first conclude that a novel stump-like mathematical model was advanced for simulation of CZE with different sample injection. Second, an innovative computer program was developed which relied on the model and other physico-chemical parameters. Third, the developed software can simulate both Gaussian and plateau concentration distribution peaks, and simulate both final electropherogram of CZE and dynamic progress of separation in CZE. Fourth, the relevant experiments were performed and compared with the simulation results, highly demonstrating the validity of the developed mathematical model and its relevant program. Fifth, the simulation results of electropherogram of 20 amino acids via the developed software were compared with those by the popular software PeakMaster, revealing the consistency of electromigration time and peak sequence between the two softwares. The obvious advantage of the developed software was the dynamics and plateau peak simulation which explained the separation progress and the emergence of plateau peak in CZE. In addition, this software provides a friendly visual interface which makes users operate easily, and it has no special requirements on hardware.

Of course, the developed software can only simulate the simplest separation of zone electrophoresis in CZE. The developed mathematical models were obviously simplified (such as diffusion coefficient model), and some other factors were not taken into account. Therefore, we plan to develop a versatile software program which will overcome those issues and improve the relevant function in the future.

Acknowledgments

The authors are grateful for the funding provided by the National Natural Science Foundation of China (nos. 21035005 and 21275099), National Key Program of Scientific Instrument Development (no. 2011YQ030139), and Shanghai Jiao Tong University.

Appendix A. Supporting information

Supplementary data associated with this article can be found in the online version at http://dx.doi.org/10.1016/j.talanta.2012.10.010.

References

[1] R.A. Mosher, D.A. Saville, W. Thormann, The Dynamics of Electrophoresis, VCH, Cambridge, 1992.
[2] J.L. Beckers, F.M. Everaerts, J. Chromatogr. 68 (1972) 207.
[3] T. Hirokawa, N. Aoki, Y. Kiso, J. Chromatogr. 312 (1984) 11.
[4] P. Radi, E. Schumacher, Electrophoresis 8 (1985) 195.
[5] K. Shimao, Electrophoresis 7 (1986) 121.
[6] K. Shimao, Electrophoresis 7 (1986) 297.
[7] J. Heinrich, H. Wagner, Electrophoresis 13 (1992) 44.

[8] J. Caslavska, T. Kaufmann, P. Gebauer, W. Thormann, J. Chromatogr. 638 (1993) 205.
[9] C. Schafer-Nielsen, Electrophoresis 16 (1995) 1369.
[10] C. Schwer, B. Gas, F. Lottspeich, E. Kenndler, Anal. Chem. 65 (1993) 2108.
[11] V. Hruska, M. Jaros, B. Gas, Electrophoresis 27 (2006) 984.
[12] A. Murel, I. Kirjanen, O. Kirret, J. Chromatogr. 174 (1979) 1.
[13] M. Bier, R.A. Mosher, O.A. Palusinski, J. Chromatogr. 211 (1981) 313.
[14] W. Thormann, R.A. Mosher, M. Bier, J. Chromatogr. 351 (1986) 17.
[15] R.A. Mosher, W. Thormann, M. Bier, J. Chromatogr. 351 (1986) 31.
[16] Q.L. Mao, J. Pawliszyn, W. Thormann, Anal. Chem. 72 (2000) 5493.
[17] R.A. Mosher, W. Thormann, Electrophoresis 23 (2002) 1803.
[18] W. Thormann, T.M. Huang, J. Pawliszyn, Electrophoresis 25 (2004) 324.
[19] W. Thromann, R.A. Mosher, Electrophoresis 27 (2006) 968.
[20] K. Shimao, Electrophoresis 8 (1987) 14.
[21] K. Shimao, Jpn. J. Electrophoresis 38 (1994) 221.
[22] K. Shimao, Jpn. J. Electrophoresis 38 (1994) 417.
[23] J. Jin, J. Shao, S. Li., W. Zhang, L.Y. Fan, C.X. Cao, J. Chromatogr. A 1216 (2009) 4913.
[24] Y.J. Xu, S. Li, W. Zhang, L.Y. Fan, J. Shao, C.X. Cao, J. Sep. Sci. 32 (2009) 585.
[25] J.C. Reijenga, E. Kenndler, J. Chromatogr. A 659 (1994) 417.
[26] A. Cifuentes, H. Poppe, J. Chromatogr. A 680 (1994) 321.
[27] G.M. Janini, C.J. Metral, H.J. Issaq, G.M. Muschik, J. Chromatogr. A 848 (1999) 417.
[28] B. Gas, M. Stedry, A. Rizzi, E. Kenndler, Electrophoresis 16 (1995) 958.
[29] M. Stedry, M. Jaros, B. Gas, J. Chromatogr. A 960 (2002) 187.
[30] G.L. Erny, E.T. Bergstrom, D.M. Goodall, J. Chromatogr. A 959 (2002) 229.
[31] M.Y. Hsu, C.I. Hung, Jpn. J. Appl. Phys. 46 (Part 1) (2007) 3605.
[32] V. Hruska, M. Riesova, B. Gas, Electrophoresis 33 (2012) 923.
[33] M. Riesova, V. Hruska, B. Gas, Electrophoresis 33 (2012) 931.
[34] G.L. Erny, E.T. Bergstrom, D.M. Goodall, Anal. Chem. 73 (2001) 4862.
[35] W. Friedl, J.C. Reijenga, E. Kenndler, J. Chromatogr. A 709 (1995) 163.
[36] C.X. Cao, J. Chromatogr. A 771 (1997) 375.
[37] X. Huang, J.A. Luckey, M.J. Gorden, R.N. Zare, Anal. Chem. 61 (1989) 766.
[38] D.J. Rose, J.W. Jorgenson, Anal. Chem. 60 (1988) 642.
[39] N.V. Komarova, J.S. Kamentsev., J. Chromatogr. B 800 (2004) 135.